Measurement of jet substructure and jet fragmentation using the ATLAS detector

Javier Llorente
on behalf of the ATLAS Collaboration.

Simon Fraser University

DIS 2021 - April 14, 2021

Outline of the talk

Several measurements of jet fragmentation and substructure recently released:

- Jet fragmentation using charged particles [PRD 100, 052011 (2019)]
- Soft-drop jet observables [PRD 101, 052007 (2020)]
- Lund jet plane using charged particles [PRL 124, 222002 (2020)]

Motivation for such measurements

- Sensitive to parton shower and fragmentation models in MC simulations.
- Compare to resummed theoretical predictions beyond leading logarithm.
- Gain understanding in quark/gluon jet separation
  - Interesting from the theoretical point of view.
  - Experimentally useful to reduce JES uncertainties in both ATLAS and CMS.

Jet fragmentation using charged particles [PRD 100, 052011 (2019)]

- At least two anti-k_t jets ($R = 0.4$) with $p_T > 60$ GeV and $|\eta| < 2.1$.
- Dijet p_T balance: $p_T^{(1)}/p_T^{(2)} < 1.5$ (enhancing $2 \to 2$ topologies).
- Charged particles within the jet with $p_T > 50$ MeV, $|\eta| < 2.5$ are selected.
- Two jet subsets: most central and most forward among the two leading.

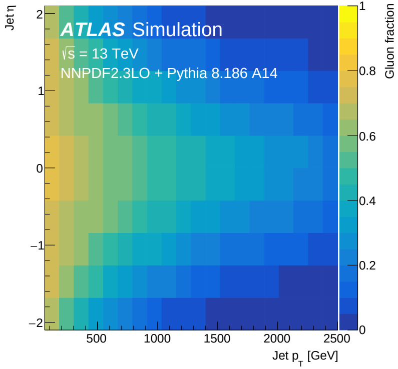

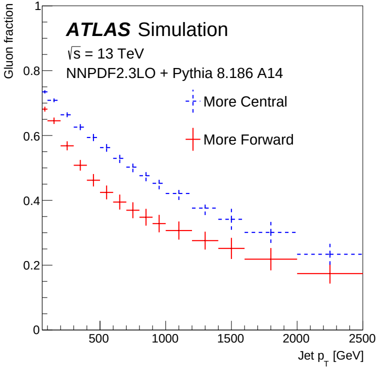

Central jets are more likely to arise from gluon fragmentation.

Measurement of observables sensitive to the fragmentation functions

- Number of charged particles $\langle n_{\rm ch} \rangle$ in jet.
- Momentum fraction $\zeta = p_T^{\rm ch}/p_T^{\rm jet}$.
- Transverse profile $p_T^{\rm rel} = p_T^{\rm ch} \sin\theta_{jc}$.
- Radial profile $\rho = 1/(2\pi r N_{\rm jet}) dn_{\rm ch}/dr; \quad r = \Delta R_{jc}$.

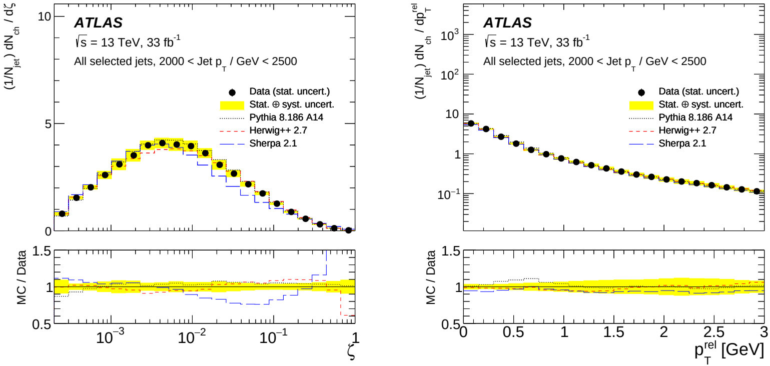

Jet fragmentation using charged particles [PRD 100, 052011 (2019)]

The average values of the observables are presented as a function of the jet p_T.

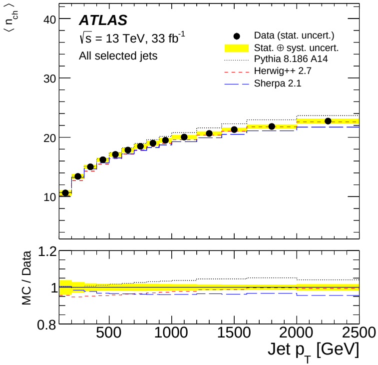

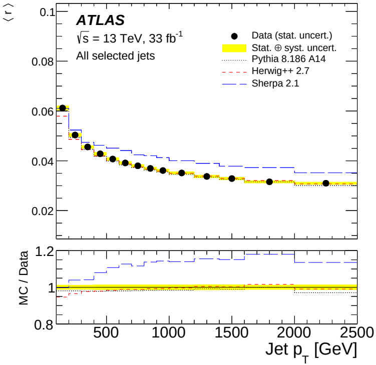

- Data to MC disagreements observed in some regions of the phase space.
- SHERPA 2.1 fails to describe the r data at high p_T.
- Radial profile is systematically broader in SHERPA than in data, although description is more reasonable for other observables.

Distributions are obtained separately for more central and more forward jets

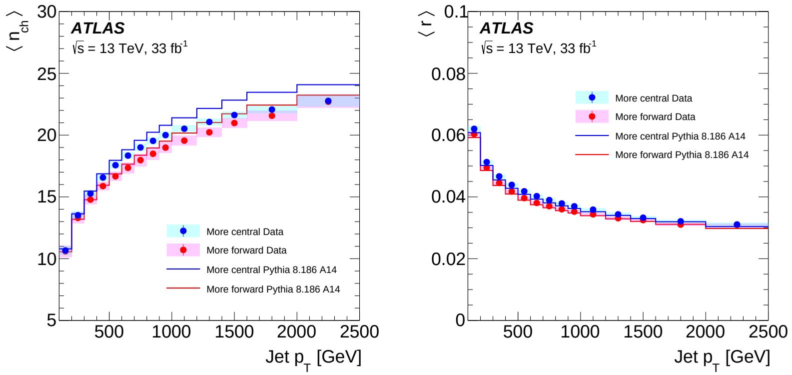

- $\langle n_{\mathrm{ch}} \rangle$ is clearly larger for central jets, as well as $\langle r \rangle$.
- Gluon jets contain more charged particles, and are wider than quarks.

Quark and gluon-like distributions obtained by solving a linear system of equations for bin i of each observable (with model-dependent coefficients).

$$\left.\begin{aligned} h_i^f &= f_q^f h_i^q + (1 - f_q^f) h_i^g \\ h_i^c &= f_q^c h_i^q + (1 - f_q^c) h_i^g \end{aligned}\right\}$$

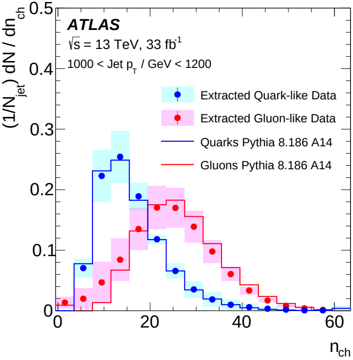

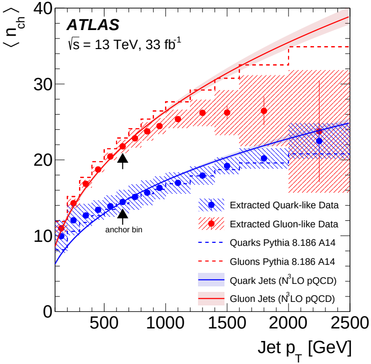

- $\langle n_{\rm ch} \rangle$ versus p_T is compared to N^{3}LO predictions.
- Theory predicts higher values of $\langle n_{\rm ch} \rangle$ at high p_T than observed.
- Pythia prediction overestimates $\langle n_{\rm ch} \rangle$ for gluon jets.

The so-called 'jet topic' approach does not involve model-dependent flavour composition fractions. Quark and gluon-like jet topics are defined as

$$h_i^{T_1} = \frac{h_i^f - \min_j\{h_j^f/h_j^c\} \times h_i^c}{1 - \min_j\{h_j^f/h_j^c\}}; \qquad h_i^{T_2} = \frac{h_i^c - \min_j\{h_j^c/h_j^f\} \times h_i^f}{1 - \min_j\{h_j^c/h_j^f\}}$$

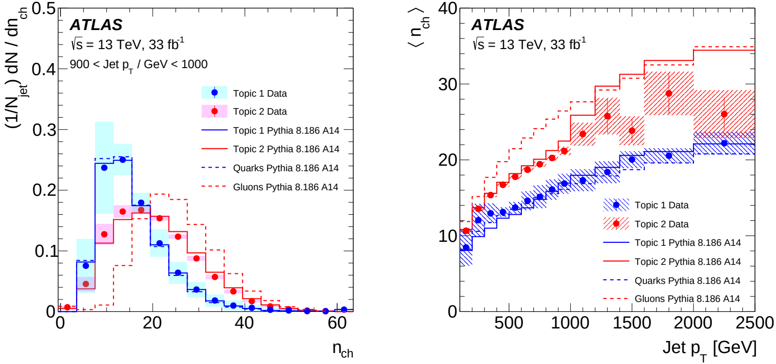

- Topic 1 agrees well with quark-like jet simulation
- Topic 2 differs from gluon-like jet simulation, which predicts higher $\langle n_{\mathrm{ch}} \rangle$

Soft-drop jet observables [PRD 101, 052007 (2020)]

- Dijet (anti-k_t, $R = 0.8$) events with $p_{T1}/p_{T2} < 1.5$ are selected..
- Two inputs for jet substructure: clusters and tracks ($p_T > 500$ MeV).
- Constituents (tracks, clusters) are reclustered using C/A algorithm.
- The last step of the clustering is undone, producing subjets 1 and 2.
- Subjets 1 and 2 are evaluated using the soft-drop condition:

$$\frac{\min(p_{T1}, p_{T2})}{p_{T1} + p_{T2}} > z_{\mathrm{cut}} \left(\frac{\Delta R_{12}}{R} \right)^{\beta}$$

- Remove the lower p_T subjet and iterate until the condition is fulfilled.

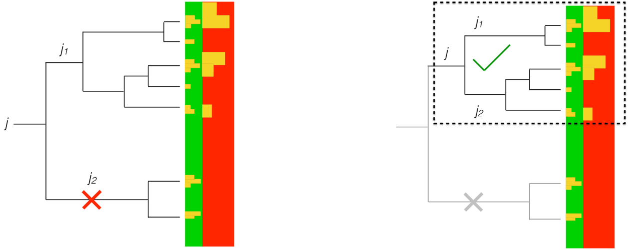

Soft-drop jet observables [PRD 101, 052007 (2020)]

- Measurements are performed for SD parameters $z_{\text{cut}} = 0.1$ and $\beta = 0, 1, 2$.
- Higher values of β imply larger non-perturbative effects.

Dimensionless mass: $\rho = \log\left(\frac{m^2}{p_T^2}\right)$, where $m^2 = \left(\sum_{i=1}^{N} E_i\right)^2 - \left(\sum_{i=1}^{N} \vec{p}_i\right)^2$

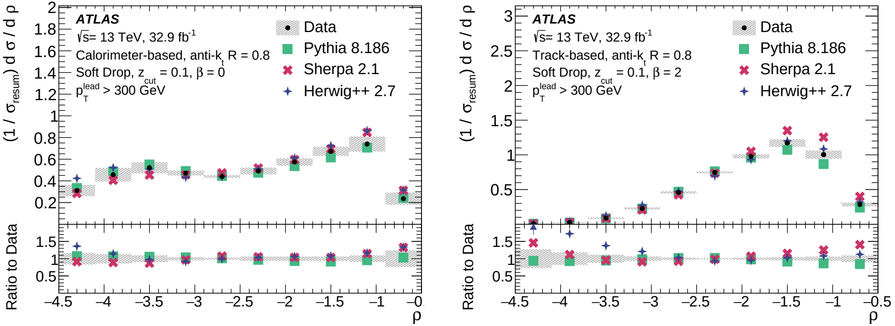

Soft-drop jet observables [PRD 101, 052007 (2020)]

- Measurements are performed for SD parameters $z_{\text{cut}} = 0.1$ and $\beta = 0, 1, 2$.
- Higher values of β imply larger non-perturbative effects.

$$\text{Splitting scale for subjet fulfilling SD: } z_g = \frac{\min(p_{T1}, p_{T2})}{p_{T1} + p_{T2}}$$

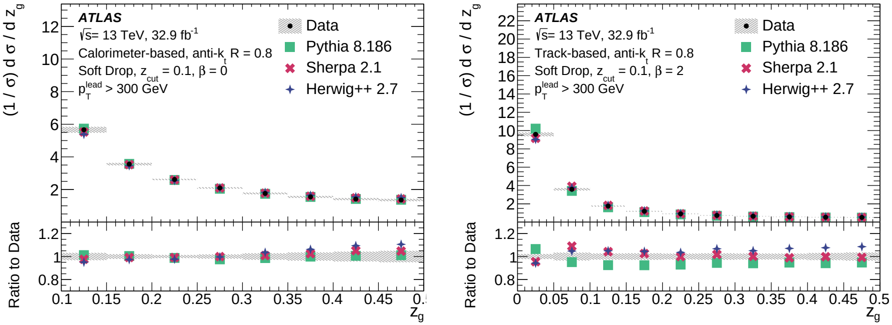

Soft-drop jet observables [PRD 101, 052007 (2020)]

- Measurements are performed for SD parameters $z_{\mathrm{cut}} = 0.1$ and $\beta = 0, 1, 2$.
- Higher values of β imply larger non-perturbative effects.

Angular distance for subjet fulfilling SD: $r_g = \sqrt{(y_1 - y_2)^2 + (\phi_1 - \phi_2)^2}$

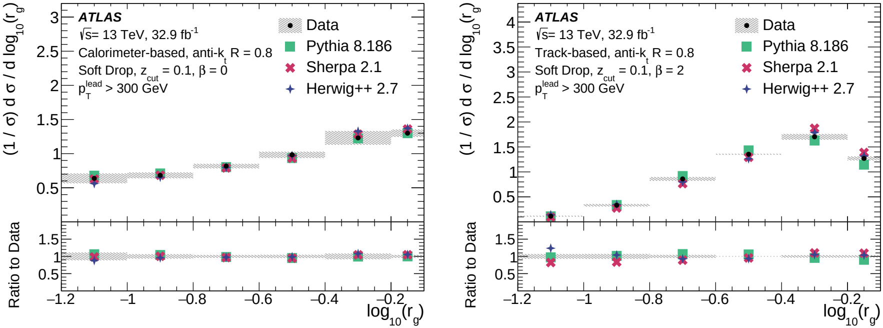

Comparison with analytical predictions (+non-perturbative corrections)

- LO+NNLL and NNLL based on SCET [hep-ph/0011336, hep-ph/0109045]
- NLO + NLL matched to NLOJet++ (+ z_{cut} resummation).

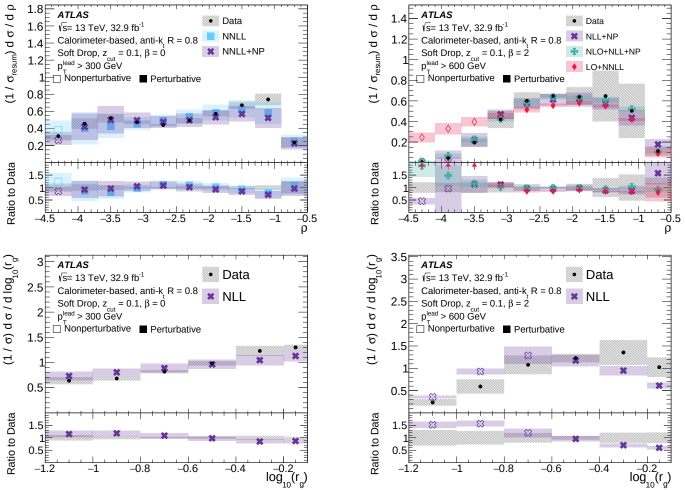

- Comparison between track and cluster observables.
- Distributions of ρ for $\beta = 0$ and $\beta = 2$.
- Overall, $\beta = 0$ presents a better agreement between both observables.

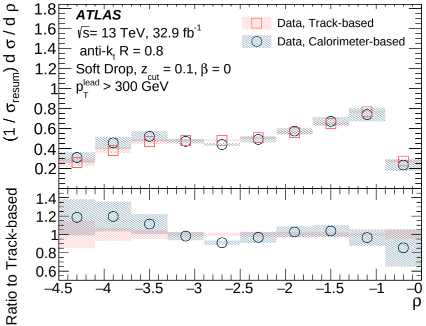

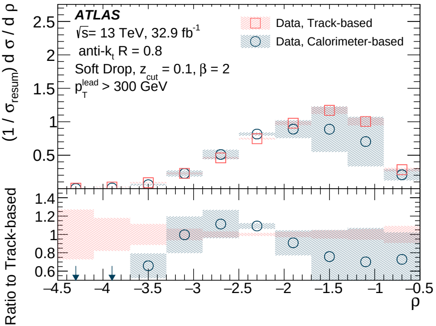

Quark and gluon distributions obtained by solving a per-bin system of equations

$$\left.\begin{aligned} h_i^f &= f_q^f h_i^q + (1 - f_q^f) h_i^g \\ h_i^c &= f_q^c h_i^q + (1 - f_q^c) h_i^g \end{aligned}\right\}$$

As expected, gluon jets are more massive and wider than quark jets.

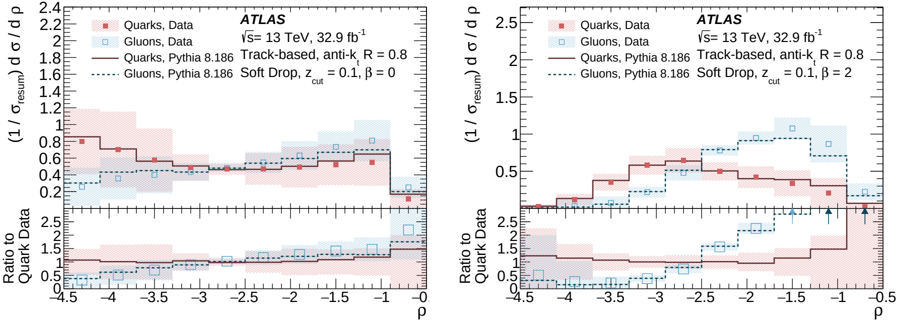

Lund jet plane using charged particles [PRL 124, 222002 (2020)]

Differential cross-section versus splitting fraction (z) and emission angle (ΔR).

- Dijet (anti-k_t, $R = 0.4$) events are selected with $p_T^{(1)}/p_T^{(2)} < 1.5$.
- Tracks within $\Delta R = 0.4$ of jet axis are reclustered using C/A algorithm.
- The clustering history is examined, z and ΔR obtained for each splitting.

$$z = \frac{p_{T2}}{p_{T1} + p_{T2}}; \qquad \Delta R = \sqrt{(y_1 - y_2)^2 + (\phi_1 - \phi_2)^2}$$

- Featuring a flat perturbative region sensitive to PS effects (hard, wide-angle) below hadronisation-sensitive diagonal ($k_t \simeq \Lambda_{\mathrm{QCD}}$).

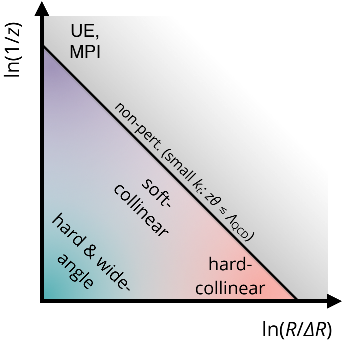

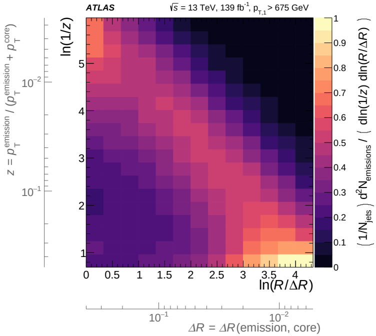

Lund jet plane using charged particles [PRL 124, 222002 (2020)]

Sensitivity to the ME calculation, parton shower and hadronisation models.

<u>Parton shower</u>

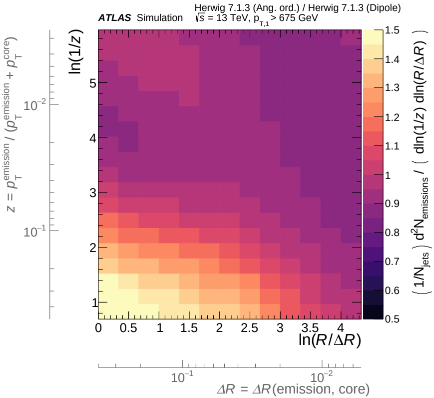

<u>Hadronisation model</u>

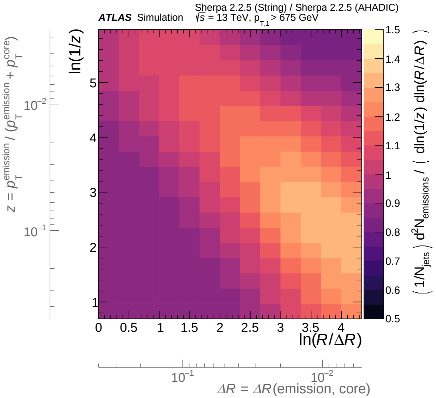

- The plots show the ratios for different shower and hadronisation models.
- Angle-ordered PS presents more hard, wide angle activity than dipole PS.
- String model presents more hard collinear activity than cluster model.

The plane is also presented in horizontal and vertical slices

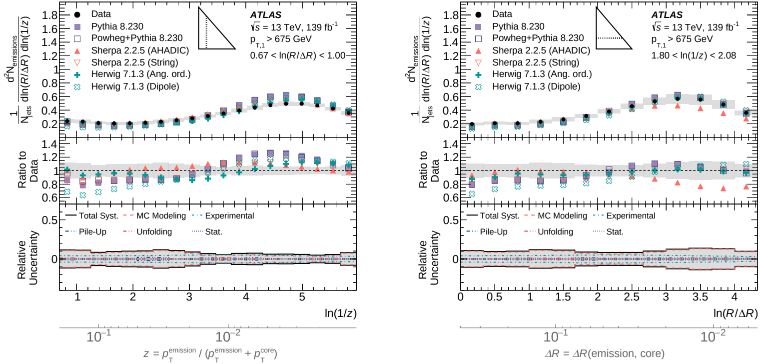

- No MC prediction provides an accurate description of all regions.
- HERWIG with angle-ordered shower gives the best overall agreement.
- Both HERWIG models differ most for hard emissions at wide angles.
- POWHEG+PYTHIA differs with PYTHIA for the hardest, wide-angle emissions, where the ME calculation is relevant.

Summary and conclusions

- Measurements of jet fragmentation and substructure are presented.
  - Jet variables sensitive to the fragmentation functions.
  - Observables for SD-groomed jets (mass, splitting scale, angular opening).
  - Lund jet plane: Splitting fraction versus angular opening.
- Quark and gluon-like jet distributions extracted using central/forward jets.
- Comparison with MC predictions over a large phase space.
- HepData and Rivet routines are available for the presented measurements.
- Stay tuned for more measurements to be released soon!